










# Unraveling the physical information of depolarizers

ALBERT VAN EECKHOUT,<sup>1,\*</sup>  JOSE J. GIL,<sup>2</sup>  ENRIQUE GARCIA-CAUREL,<sup>3</sup>  JAVIER GARCÍA ROMERO,<sup>1</sup> RAZVIGOR OSSIKOVSKI,<sup>3</sup>  IGNACIO SAN JOSÉ,<sup>4</sup> IGNACIO MORENO,<sup>5</sup>  JUAN CAMPOS,<sup>1</sup>  AND ANGEL LIZANA<sup>1</sup> 

<sup>1</sup>Grup d'Òptica, Physics Department, Universitat Autònoma de Barcelona, Bellaterra, Spain

<sup>2</sup>Department of Applied Physics, University of Zaragoza, Zaragoza, Spain

<sup>3</sup>LPICM, CNRS, Ecole polytechnique, Institut Polytechnique de Paris, Palaiseau, France

<sup>4</sup>Instituto Aragonés de Estadística, Gobierno de Aragón, Zaragoza, Spain

<sup>5</sup>Departamento de Ciencia de Materiales, Óptica y Tecnología Electrónica, Universidad Miguel Hernández de Elche, Elche, Spain

\*[albert.vaneckhout@uab.cat](mailto:albert.vaneckhout@uab.cat)

**Abstract:** The link between depolarization measures and physical nature and structure of material media inducing depolarization is nowadays an open question. This article shows how the joint use of two complementary sets of depolarizing metrics, namely the Indices of polarimetric purity and the Components of purity, are sufficient to completely describe the integral depolarizing properties of a sample. Based on a collection of illustrative and representative polarimetric configurations, a clear and meaningful physical interpretation of such metrics is provided, thus extending the current tools and comprehension for the study and analysis of the depolarizing properties of material media. This study could be of interest to those users dealing with depolarization or depolarizing samples.

© 2021 Optical Society of America under the terms of the [OSA Open Access Publishing Agreement](#)

## 1. Introduction

The fundamental understanding of light scattering phenomena is of interest in scientific and technological fields as diverse as astronomy, remote sensing, metrology and biomedical imaging, among others [1–13]. In particular, the study of light depolarization processes finds a very wide scope of applications, for instance, the characterization of gaseous structures in the cosmos [3,4], remote sensing of diffuse objects [1], and the early diagnosis of diseases [5,8,9].

Some intrinsic structural information of scattering media can be inferred from light depolarization measurements. Such measurements give a macroscopic view of the random scattering process, connected with the physical properties of materials and with light-matter interactions. Nowadays, different depolarization metrics are available in the literature [14–25] for the analysis of the different aspects of scattered light, such as randomness, entropy, or degree of polarization, among others. However, the link between depolarization measures through different metrics and the physical properties of the sample involved in such depolarization values is a challenging topic that is still under investigation.

Commonly, the depolarization properties of scattering media are inspected by using the so-called depolarization index,  $P_{\Delta}$  [14]. The depolarization index,  $P_{\Delta}$ , is a generalization of the degree of polarization (DoP), but instead of characterizing light beams like DoP,  $P_{\Delta}$  is a measure of the depolarizing power of a material medium. In particular,  $P_{\Delta}$  quantifies the randomness of the processes behind the scattering interactions but does not discriminate their different physical origins that contribute to the overall depolarization.

To get a more accurate description of the depolarization phenomena, it is necessary to use a complete set of polarization descriptors rather than just a single parameter. With this aim,

some authors proposed to combine  $P_{\Delta}$  with another metric called the overall purity index PI [22]. PI is a global descriptor of depolarization, like  $P_{\Delta}$ , that exhibits an alternative measure of the overall depolarization, and which is compatible with  $P_{\Delta}$ . Although the combined use of PI and  $P_{\Delta}$  improves the description of the depolarization phenomena, their combined use does not provide a complete description of the depolarization structure of the medium. Therefore, other descriptors must be explored to get a more accurate description of the depolarization structure of the medium.

Under the common assumption of linearity of the polarimetric response of a given medium, the sixteen elements of the Mueller matrix  $\mathbf{M}$  encode, in an intricate manner, all information on the response in question. Therefore, all the physical properties of the sample producing some kind of polarimetric response cannot be directly described from the  $\mathbf{M}$  coefficients [26]. To this aim, some of the multiple Mueller decompositions can be applied.

By means of the *arrow decomposition* approach [27,28], it has been proven that  $\mathbf{M}$  can be factored as the product of three matrices, namely two retarders, which are respectively multiplied to the right (entry retarder) and to the left (exit retarder) of a depolarizer without retardance that accumulates the entangled information on polarizance, diattenuation and depolarization. Thus, the physical information provided by  $\mathbf{M}$  can be considered as composed of, a) three parameters that determine the entrance retarder (in general elliptical); b) three parameters that determine the exit retarder (in general elliptical); c) four angular parameters determining the direction of the diattenuation and polarizance vectors; d) the  $\mathbf{M}$  element  $m_{00}$  and e) five remaining parameters relative to diattenuation  $D$ , polarizance  $P$  and depolarization [27,28].

In this work, we study in detail two groups of different metrics, the Indices of Polarimetric Purity (IPP) [20] and the Components of Purity (CP) [21], that are connected to the well-known and commonly used depolarization index  $P_{\Delta}$  [14] and which provide together complete information on the integral depolarization properties of media [27]. Their physical meaning, as well as their complementary use for the complete analysis of the scattering phenomena, is discussed through a collection of illustrative and easy to interpret examples.

## 2. Mathematical description of $P_{\Delta}$ , CP, and IPP

In the following section, we summarize the main mathematical foundations of  $P_{\Delta}$ , IPP and CP, which are the metrics inspected in this work. Moreover, we provide a visual and intuitive physical description for their better understanding. This section also shows the fundamental relation between the different groups of parameters (IPP and CP) and  $P_{\Delta}$ .

### 2.1. Depolarization index ( $P_{\Delta}$ )

$P_{\Delta}$  can be directly calculated from the elements of the  $4 \times 4$   $\mathbf{M}$  describing the interaction of light with the sample [14,29]:

$$P_{\Delta} \equiv \sqrt{\frac{1}{3m_{00}^2} \left( \sum_{i,j=0}^3 m_{ij}^2 - m_{00}^2 \right)} = \sqrt{\frac{1}{3} \left( \frac{1}{m_{00}^2} \text{tr}(\mathbf{M}^T \mathbf{M}) - 1 \right)}, \quad (1)$$

where  $m_{ij}$  is the element at the  $i$ -th row and  $j$ -th column of  $\mathbf{M}$ ,  $m_{00}$  is interpreted as the mean intensity transmittance or reflectance of the sample for unpolarized light [29] and  $\text{tr}$  is the matrix trace.  $P_{\Delta}$  is a global measure of the depolarization behavior. Its maximum value, associated with a non-depolarizing medium, is 1 whereas its minimum value, attained by a totally depolarizing medium, is 0.

### 2.2. Components of Purity (CP)

The Components of Purity, CP, is a group of three parameters that arise from the link between the depolarization properties of scattering media and their dichroism. As a result, two of the

three CP parameters are the polarizance  $P$  (the absolute value of the polarizance vector [26]) and the diattenuation  $D$  (the absolute value of the diattenuation vector [26]).

$$P = \sqrt{\frac{\sum_{i=1}^3 m_{i0}^2}{m_{00}^2}}, \quad D = \sqrt{\frac{\sum_{j=1}^3 m_{0j}^2}{m_{00}^2}}. \quad (2)$$

From a squared and expanded definition of  $P_{\Delta}$  [21], we can directly relate  $P_{\Delta}$  with  $P$  and  $D$ :

$$P_{\Delta}^2 = \frac{\sum_{i=1}^3 m_{i0}^2}{3m_{00}^2} + \frac{\sum_{j=1}^3 m_{0j}^2}{3m_{00}^2} + \frac{\sum_{i,j=1}^3 m_{ij}^2}{3m_{00}^2}, \quad (3)$$

$$P_{\Delta}^2 = \frac{1}{3}P^2 + \frac{1}{3}D^2 + P_s^2, \quad (4)$$

where  $P_s$  is the third CP parameter defined as [21]:

$$P_s = \sqrt{\frac{\sum_{i,j=1}^3 m_{ij}^2}{3m_{00}^2}}. \quad (5)$$

$P$ ,  $D$ , and  $P_s$  are the three CP components. They take values in the range  $[0,1]$ , but can never be all three equal to one. The latter follows from the  $P_{\Delta}$ -range limitation ( $0 \leq P_{\Delta} \leq 1$ ).

The depolarization, which eventually appears in the polarimetric measurement of the optical response of any physical system, arises from the incoherent composition of the contributions associated with the dichroic and birefringent elementary effects. Therefore, by analyzing Eq. (4), we realize that the overall depolarizing properties derived from the incoherent composition of birefringent effects in the sample are encoded into the  $P_s$  parameter. Note that each depolarizer featuring a given  $P_{\Delta}$  value, has three values for the CP, so it can be represented in a new tridimensional space (we label it as the  $P$ - $D$ - $P_s$  space; see Fig. 1) where  $P$ ,  $D$  and  $P_s$  are the coordinates of an orthogonal coordinate system.

Regardless of the depolarization complexity, each existing depolarizer can be represented in the  $P$ - $D$ - $P_s$  space (Fig. 1) by using a single point. The coordinates of such point in the  $P$ - $D$ - $P_s$  space determine the polarizance-diattenuation (dichroism) and the  $P_s$  contributions involved in the depolarizing process. Importantly, the points in the  $P$ - $D$ - $P_s$  space related to a constant value of  $P_{\Delta}$  lie on the surface of an ellipsoid defined by Eq. (4). The whole ellipsoid cannot be fully represented because only a portion of it is comprised within the domain of values pertaining to the  $P$ - $D$ - $P_s$  space ( $P^2 + D^2 \leq 1 + 3P_s^2$ ) [21]. The latter is of relevant significance because depolarizers with very different intrinsic origins but leading to the same overall depolarization ( $P_{\Delta}$ ), are clearly discriminated in the  $P$ - $D$ - $P_s$  space as points located at different positions upon the same surface. As an example, different surfaces with a constant  $P_{\Delta}$  are represented in Fig. 1. It is worth noting that the higher the value of  $P_{\Delta}$ , the larger the area covered by the corresponding surface (the smallest one corresponds to  $P_{\Delta}=0$  while the largest one, to  $P_{\Delta}=1$ ). Accordingly, the discriminating potential of the CPs is higher for low depolarizing systems.

A planar representation of this purity figure (Fig. 1) with axes  $P_s$  and  $P_p$  ( $P_p$  being the *degree of polarizance*  $P_p = \sqrt{(P^2 + D^2)/2}$ ) was studied in [21,27]. Such representation is characterized for taking the dichroism information in a unique parameter  $P_p$  thus reducing the dimensionality of the figure. This dimensionality reduction allows the performance of new 3D spaces that includes new information about the statistical nature of the random processes behind the scattering interactions

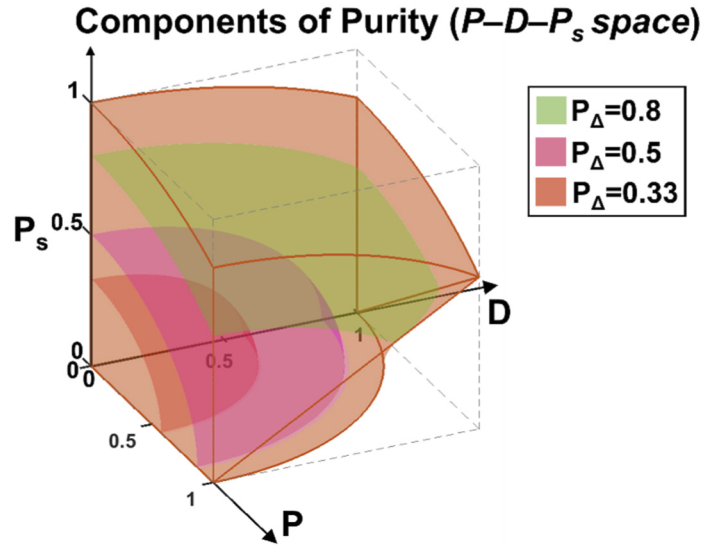


**Fig. 1.** Representation of the  $P$ - $D$ - $P_s$  space . Each surface drawn with a different color corresponds to a different value of  $P_{\Delta}$ .

in the system, e.g., the PI-CP space discussed in Ref. [23]. However, these new spaces lose the  $P$ - $D$  discrimination information and consequently, some  $\mathbf{M}$  cannot be differentiated. For example, the forward and reverse  $\mathbf{M}$ , discussed in the next section 3, cannot be differentiated when using  $P_p$  instead of  $P$  and  $D$

### 2.3. Indices of Polarimetric Purity (IPP)

A complementary view of the depolarization is given by the so-called Indices of Polarimetric Purity (IPP) whose contributions to overall depolarization are irrespective of the nature of the polarimetric phenomena involved (unlike those of the CP, which depend on diattenuation, polarizance, and  $P_s$ ) but only depend on the relative weights of the incoherent components of the sample. The IPP are three parameters defined as follows [20]:

$$P_i \equiv \frac{1}{m_{00}} \sum_{k=1}^i k(\lambda_{k-1} - \lambda_k) \quad (6)$$

where  $i = 1, 2, 3$  and  $\lambda_k$  are the eigenvalues of the covariance matrix  $\mathbf{H}(\mathbf{M})$  taken in decreasing order [15,26]. The latter is defined from a linear transformation of the elements of  $\mathbf{M}$  required for applying the Spectral Decomposition of  $\mathbf{M}$  [15,26],

$$\mathbf{H}(\mathbf{M}) \equiv \frac{1}{4} \sum_{i,j=0}^3 m_{ij}(\sigma_i \otimes \sigma_j^*), \quad (7)$$

where  $\otimes$  denotes the Kronecker product while  $\sigma_0$  is the  $2 \times 2$  identity matrix and  $\sigma_i$ ,  $i = 1, 2, 3$  are the Pauli matrices.

In order to link IPP parameters with  $P_{\Delta}$ , it is necessary to reformulate Eq. (7) in the following way:

$$m_{ij} = \text{tr}[(\sigma_i \otimes \sigma_j^*)\mathbf{H}(\mathbf{M})]. \quad (8)$$

The properties of the trace help to express  $P_{\Delta}$  in terms of a combination of the eigenvalues ( $\lambda_i$ ). For that purpose, we first use Eq. (8) to link the elements  $m_{ij}$  of  $\mathbf{M}$  with  $\lambda_i$  as follows [30]:

$$\sum_{i,j=0}^3 m_{ij}^2 = 4 \sum_{i=0}^3 \lambda_i^2. \tag{9}$$

Secondly, from Eq. (7) it is possible to write the trace of  $\mathbf{H}$  in terms of  $\lambda_i$  and  $m_{00}$ .

$$\text{tr}(\mathbf{H}) = m_{00} = \sum_{i=0}^3 \lambda_i \tag{10}$$

The combination of Eqs. (9) and (10) leads to [30]:

$$P_{\Delta} = \sqrt{\frac{4 \sum_{i=0}^3 \lambda_i^2 - \left(\sum_{i=0}^3 \lambda_i\right)^2}{3 \left(\sum_{i=0}^3 \lambda_i\right)^2}} \tag{11}$$

Finally,  $\lambda_i$  can be substituted in the proceeding expression by the corresponding IPP (Eq. (6)) giving [20]:

$$P_{\Delta}^2 = \frac{2}{3}P_1^2 + \frac{2}{9}P_2^2 + \frac{1}{9}P_3^2 \tag{12}$$

Conversely to what happens with the CP, it may occur that more than one IPP is equal to one, which corresponds to particular points in the corresponding IPP space. In fact,  $P_1 = P_2 = P_3 = 1$  corresponds to a non-depolarizing sample, whereas  $P_1 = P_2 = P_3 = 0$  represents an ideal perfect depolarizer. As in the case of CP, the IPP can be represented in a 3D space associating each parameter with an axis. This visual representation has been previously described in the literature [20] and corresponds to the IPP space also called *Purity Space*.

### Indices of Polarimetric Purity (*Purity Space*)

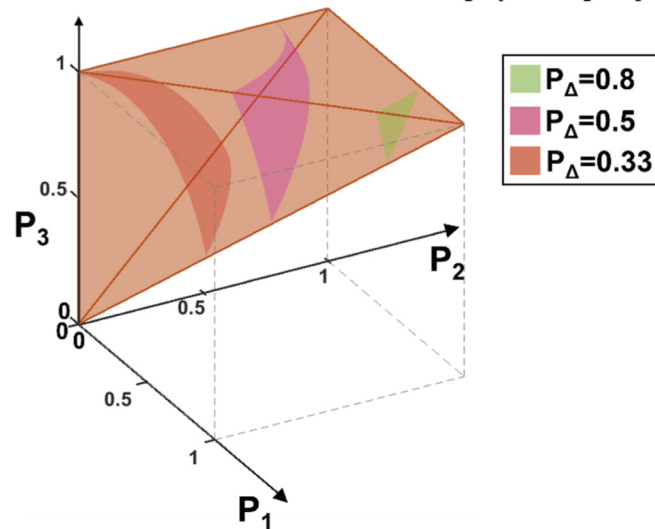


**Fig. 2.** Representation of the IPP space. Each surface drawn with a different color is associated with a different value of  $P_{\Delta}$ .

For the sake of visualization, the IPP space is represented in Fig. 2, where any physically realizable depolarizer is comprised within a tetrahedron, which is defined by the inherent constraint obeyed by the IPP:  $0 \leq P_1 \leq P_2 \leq P_3 \leq 1$ . As in the case of the  $P$ - $D$ - $P_S$  space, constant values of  $P_A$  are represented by surfaces in the IPP space. To go further, it is worth mentioning that, according to Eq. (12), constant values of  $P_A$  describe the surface of an ellipsoid with  $P_1$ ,  $P_2$  and  $P_3$  as parameters, limited by the indicated constraint  $0 \leq P_1 \leq P_2 \leq P_3 \leq 1$ . Note that, unlike in the  $P$ - $D$ - $P_S$  space, in the IPP space the area of the surface does not necessarily decrease as  $P_A$  decreases. In fact, the largest surface is associated with  $P_A=1/3$ .

### 3. Physical interpretation and complementarity of CP and IPP

The above-discussed transformation of a single overall value ( $P_A$ ) to two mutually complementary 3D spaces allows synthesizing the depolarizing information of the sample to a new basis with richer physical interpretation, because each new parameter provides specific information on the sample. In that sense, CP are sensitive to the way in which depolarization is related to the nature of the polarimetric behavior of the probed medium, resulting from the averaged effects of diattenuation, polarizance and retardance. Unlike CP, the IPP are insensitive to the nature of the components integrating  $\mathbf{M}$ ; that is, the IPP do not carry information on specific diattenuation, polarizance or retardation properties of the medium represented by  $\mathbf{M}$  [27], but rather result from the structure of polarimetric randomness of the sample (as in other related works, with polarimetric randomness we refer to the lack of determinism of the polarimetric properties exhibited by  $\mathbf{M}$ ), which is determined by the relative weights of the components of the characteristic decomposition of  $\mathbf{M}$  [27,29,31]

$$\mathbf{M} = P_1 \mathbf{M}_{J0} + (P_2 - P_1)\mathbf{M}_1 + (P_3 - P_2)\mathbf{M}_2 + (1 - P_3)\mathbf{M}_{\Delta 0} \quad (13)$$

where  $\mathbf{M}_{J0}$  is the nondepolarizing component generated by the eigenvector of  $\mathbf{H}$  associated with its largest eigenvalue ( $\lambda_0$ ), while  $\mathbf{M}_1$ ,  $\mathbf{M}_2$  and  $\mathbf{M}_{\Delta 0}$  are the depolarizing components generated by respective equiprobable mixtures of the two, three and four Mueller matrices associated with the sets of two, three and four eigenvectors of  $\mathbf{H}$  [27,29,31]. The characteristic decomposition of  $\mathbf{M}$  is the Mueller-algebra version of the decomposition of a partially polarized state as an incoherent combination of a totally polarized state and an unpolarized state, in such a manner that the depolarizing component of  $\mathbf{M}$  takes the structured form  $(P_2 - P_1)\mathbf{M}_1 + (P_3 - P_2)\mathbf{M}_2 + (1 - P_3)\mathbf{M}_{\Delta 0}$ , where the two- and three-component depolarizers in Eq. (13) appear combined with the perfect depolarizer (four-component depolarizer)  $\mathbf{M}_{\Delta 0} = \text{diag}(1, 0, 0, 0)$  [31]. Note that in the case of polarized light, the relative weight of the pure component is precisely the degree of polarization (which does not encompass any information on the degrees of linear or circular polarization). Similarly, the IPP provide quantitative information on the structure of polarimetric purity-randomness of the interaction represented by  $\mathbf{M}$ . Accordingly, the IPP and the CP play complementary roles in describing the depolarization properties of the probed medium.

In order to examine the complementarity of CP and IPP, it is useful to show the explicit connection between CP and IPP parameters [27],

$$3P_{\Delta}^2 = P^2 + D^2 + 3P_s^2 = 2P_1^2 + \frac{2}{3}P_2^2 + \frac{1}{3}P_3^2 \quad (14)$$

Equation (14) shows that each one of the six parameters can be calculated from the other five. It means that the index of spherical purity  $P_S$  can readily be calculated from the set  $(P_1, P_2, P_3, D, P)$ . Note that the three IPP ( $P_1, P_2$  and  $P_3$ ) [20], provide detailed information on the structure of polarimetric purity-randomness exhibited by the sample and, together with the diattenuation  $D$  and the polarizance  $P$ , complete the above indicated five polarimetrically invariant parameters of the depolarizer. In addition, it is remarkable that other relevant parameters relative to depolarization, like the Cloude's entropy  $S$  or the overall purity index PI, can also be calculated



from the same set  $(P_1, P_2, P_3, D, P)$  [22,24,27]. This complementarity of the IPP and the CP with respect to each other is the reason why they have been chosen in this work among other sets [24] as being the most meaningful independent representation of the five parameters needed to fully represent depolarization.

The relation presented in Eq. (14) also implies that for any fixed  $P, D, P_S$  triplet there is an infinite number of solutions to Eq. (14) in the form of  $P_1, P_2,$  and  $P_3$  triplets. If we define an abstract space (the IPP space) in which  $P_1, P_2,$  and  $P_3$  represent the coordinates of a basis of three orthogonal vectors, then the solutions of Eq. (14) define the surface of the positive octant of an ellipsoid in the IPP space. Similarly, for a fixed  $P_1, P_2,$  and  $P_3$  triplet, the solutions of Eq. (14) for  $P, D, P_S$  define an elliptical surface in the respective abstract  $P$ - $D$ - $P_S$  space where  $P, D,$  and  $P_S$  are the respective coordinates.

The latter point means that when polarimetric information is entangled (collapsed) in a point in either the CP or the IPP spaces, the same information can be in principle considerably expanded (disentangled) when the same polarimetric data is represented in the complementary space, i.e., in the IPP or the  $P$ - $D$ - $P_S$  spaces respectively. Note that for fixed CP or IPP values,  $P_{\Delta}$  is also fixed. There are two extreme situations that need discussion to provide further insight into the physical interpretation of polarimetric data; they are characterized by: 1) a group of depolarizers represented by a single point in the  $P$ - $D$ - $P_S$  space but by a surface at the IPP space (different IPP); and vice versa 2) a group of depolarizers represented by a single point in the IPP space but by a surface in the  $P$ - $D$ - $P_S$  space (different CP). In the following, different depolarizing samples accomplishing these two limit situations are simulated to clearly show which properties of the sample are connected to the CP and to the IPP. We would like to emphasize that two following discussed cases are the two limiting situations in which either the IPP or the CP respectively become the ideal basis to represent depolarization effects and eventually characterize a given sample. In all other cases, both the IPP and CP are two complementary views of the depolarization process: IPP characterize the statistical structure of randomness of the depolarizer (this basis can detect depolarization anisotropies of the medium, i.e., if different input polarizations are differently depolarized) while CP characterize the effect of the polarimetric properties (diattenuation, polarizance, retardance) on the depolarization process. In general, both spaces should be used to completely characterize depolarization.

### 3.1. Simulated depolarizing systems

The following study is performed by conducting a series of simulations based on *ad hoc* polarimetric samples, which are essentially synthesized from the combination of non-depolarizing diattenuators and retarders. The simulations are based on the fact that depolarizers can always be considered as incoherent combinations of non-depolarizing elements (diattenuators and retarders) [15,32], thus simplifying the physical interpretation and the comparison between spaces of observables. Most generally, any depolarizing  $\mathbf{M}$  can be described as an incoherent sum of non-depolarizing Mueller matrices  $\mathbf{M}_i$  [15,29,32]:

$$\mathbf{M} = \sum_i \alpha_i \mathbf{M}_i \quad (15)$$

where each  $\alpha_i$  can be interpreted as the relative weight that the corresponding  $\mathbf{M}_i$  component has in the sum. In practical experiments, each  $\alpha_i$  corresponds to the portion of light intensity that falls on a given part of the sample with respect to the total intensity reaching the sample. Note that in practical experiments, the measured depolarization also depends on some illumination and detection properties, such as the illumination bandwidth [33] and the numerical aperture of the detector [34]. However, the influence of the measuring instrument on the measured depolarization is beyond the scope of this study and it is not considered in the simulation.

### 3.2. Situation I: Depolarizers with identical CP but different IPP

The first case of study is associated with depolarizers without any diattenuation or polarizance content ( $P = D = 0$ ), for which  $P_S = P_A$ . According to Eq. (14), such depolarizers, which collapse into a single point in the  $P$ - $D$ - $P_S$  space, are represented as separate points in an ellipsoid associated with the given value of  $P_S$ . The closer to  $1/3$  the value of  $P_S$ , the larger the surface, and therefore the higher the potential for the IPP in discriminating between such class of non-dichroic depolarizing samples.

Non-dichroic depolarizers with  $P = D = 0$  and  $P_S = P_A$  can be constructed, according to Eq. (15), as follows:

$$\mathbf{M} = \alpha_1 \mathbf{M}_{Air} + \alpha_2 \mathbf{M}_{H0} + \alpha_3 \mathbf{M}_{H45} + \alpha_4 (\mathbf{M}_{H45} \cdot \mathbf{M}_{H0}) \quad (16)$$

where  $\mathbf{M}_{Air}$  is the  $\mathbf{M}$  of the air (i.e., the identity matrix) while  $\mathbf{M}_{H0}$  and  $\mathbf{M}_{H45}$  are respectively, the  $\mathbf{M}$  of half wave plates with their fast axis oriented at  $0^\circ$  and  $45^\circ$  with respect to the horizontal axis of the laboratory reference frame. Different combinations of weights lead to non-dichroic depolarizers; therefore, it is possible to produce any physically realizable combination of IPP values. Consequently, Eq. (16) is a generator of depolarizers of the type  $P = D = 0$ , and  $P_S = P_A$ .

The following example illustrates the use of the generator from Eq. (16), with the depolarizers labeled as  $\mathbf{M}_A$ ,  $\mathbf{M}_B$  and  $\mathbf{M}_C$  characterized with IPP, CP and  $P_A$  values shown in Table 1 (further details are given in the Table S1 of the Supplement 1). The positions of the three depolarizers in either the IPP space and in the  $P$ - $D$ - $P_S$  space are shown in Fig. 3. Note that, in Table 1, the three depolarizers present the same value of CP and  $P_A$ , but their corresponding IPP values are significantly different. In the case of non-dichroic depolarizers,  $\mathbf{M}_A$ ,  $\mathbf{M}_B$  and  $\mathbf{M}_C$ , the differences between the corresponding IPP are connected to the polarimetric randomness structure of the sample that they represent, i.e. the weights of retarders (and air) chosen to build them. This example shows how IPP are useful to distinguish among different types of anisotropic depolarizers while CP are not able to discriminate these depolarizers because all the elements are retarders without any dichroism, an essential characteristic of the  $P$ - $D$ - $P_S$  space. It is worth noting that scattering systems with different intrinsic properties (particle's size, particle's density, refractive index, etc.) presents different depolarization anisotropies, so they are described by different IPP [10–13]. Accordingly, IPP can be used to characterize such dispersion systems effectively, as proved in the literature [10–13]. In fact, some works showed that the variation of these intrinsic properties of the system show different trajectories in the IPP space [10,11] so this 3D representation (Fig. 2) is an ideal tool for the recognition and classification of scattering media.

**Table 1. Construction equation and  $P_A$ , IPP and CP values of the A, B, C, D, E, F, G, I, J and  $J^r$  depolarizers.  $\mathbf{M}_{Air}$ : Air,  $\mathbf{M}_{H0}$ : Half wave plate oriented at  $0^\circ$ ,  $\mathbf{M}_{H45}$ : Half wave plate oriented at  $45^\circ$ ,  $\mathbf{M}_{P0}$ : Linear polarizer with transmission axis oriented at  $0^\circ$ . All angles are considered with respect to the horizontal axis of the laboratory reference frame. The superscript  $T$  indicates the transpose matrix.**

	$P_1$	$P_2$	$P_3$	$P_A$	$P$	$D$	$P_S$	Depolarizer construction
$\mathbf{M}_A$	0	1	1	0.58	0	0	0.58	$1/2 \mathbf{M}_{Air} + 1/2 \mathbf{M}_{H0}$
$\mathbf{M}_B$	0.40	0.71	1	0.58	0	0	0.58	$\frac{3+\sqrt{3}}{8} \mathbf{M}_{Air} + 1/4 \mathbf{M}_{H0} + \frac{3-\sqrt{3}}{8} \mathbf{M}_{H45}$
$\mathbf{M}_C$	0.58	0.58	0.58	0.58	0	0	0.58	$\frac{3+\sqrt{3}}{4\sqrt{3}} \mathbf{M}_{Air} + \frac{\sqrt{3}-1}{4\sqrt{3}} (\mathbf{M}_{H0} + \mathbf{M}_{H45} + \mathbf{M}_{H45} \mathbf{M}_{H0})$
$\mathbf{M}_D$	0	1	1	0.58	0.50	0.50	0.41	$2/3 \mathbf{M}_{P0} + 1/3 \mathbf{M}_{H45}$
$\mathbf{M}_E$	0.40	0.71	1	0.58	0.50	0.50	0.41	$2/3 \mathbf{M}_{P0} + 1/6 (\mathbf{M}_{H0} + \mathbf{M}_{H45})$
$\mathbf{M}_F$	0.58	0.58	0.58	0.58	0.50	0.50	0.41	$2/3 \mathbf{M}_{P0} + \frac{\sqrt{3}}{9} \mathbf{M}_{H0} + \frac{3-\sqrt{3}}{18} (\mathbf{M}_{H45} + \mathbf{M}_{H45} \mathbf{M}_{H0})$
$\mathbf{M}_G$	0.33	1	1	0.64	0.33	0.33	0.58	$1/2 \mathbf{M}_{P0} + 1/2 \mathbf{M}_{H45}$
$\mathbf{M}_I$	0.33	1	1	0.64	0.67	0.67	0.33	$4/5 \mathbf{M}_{P0} + 1/5 \mathbf{M}_{H45}$
$\mathbf{M}_J$	0.33	1	1	0.64	1	0.33	0.19	$2/3 \mathbf{M}_{P0} + 1/3 \mathbf{M}_{P0} \mathbf{M}_{H45}$
$\mathbf{M}_{J^r}$	0.33	1	1	0.64	0.33	1	0.19	$diag(1, 1, 1, -1) \cdot \mathbf{M}_J^T \cdot diag(1, 1, 1, -1)$



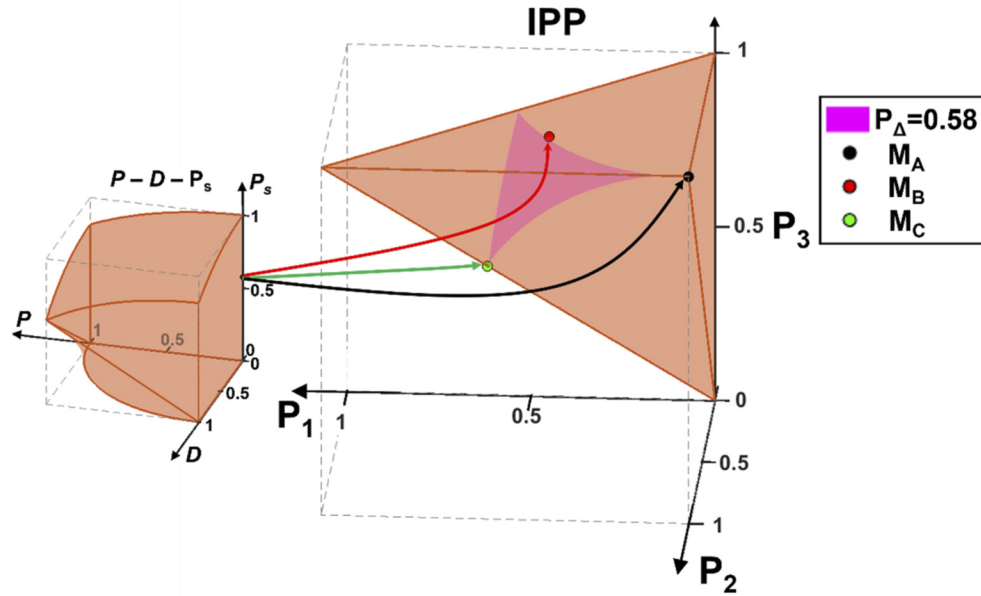


**Fig. 3.** Representation of the connection between the  $P$ - $D$ - $P_S$  space (inset) and the IPP space for the case of a group of depolarizers located on a single spot in the  $P$ - $D$ - $P_S$  space but distributed over a surface at the IPP space. The particular case of depolarizers accomplishing  $P_S = P_{\Delta} = 0.58$  is presented as an illustrative example.

Depolarizers satisfying  $D = P = 0$  belong to a more general class satisfying the condition  $D = P \geq 0$ ; for which the  $P$ - $D$ - $P_S$  space does not provide fine discrimination. For a given value of  $P_{\Delta}$ , such depolarizers have identical CP values but different IPP ones. This more general type of depolarizers can be constructed through another generator given by Eq. (17). It is similar to the one from Eq. (16) but with the matrix of a horizontal polarizer  $\mathbf{M}_{P0}$  instead of matrix  $\mathbf{M}_{Air}$ :

$$\mathbf{M}' = \alpha_1 \mathbf{M}_{P0} + \alpha_2 \mathbf{M}_{H0} + \alpha_3 \mathbf{M}_{H45} + \alpha_4 (\mathbf{M}_{H45} \cdot \mathbf{M}_{H0}) \quad (17)$$

As an example, we have synthesized three depolarizers with Mueller matrices  $\mathbf{M}_D$ ,  $\mathbf{M}_E$  and  $\mathbf{M}_F$ , characterized by the CP and IPP summarized in Table 1. Note that according to Table 1, these three examples exhibit equal CP values but different IPP. Therefore, they are seen as equivalent depolarizers with respect to the CP metrics, but they are well discriminated by using the IPP.

### 3.3. Situation II: Depolarizers with identical IPP but different CP

Now, we study another subgroup of depolarizers that satisfies the  $D = P$  condition but with different CP values and identical IPP. In contrast to the previously discussed case where the two studied depolarizers show identical diattenuation-polarizance (i.e.,  $D(\mathbf{M}_p) = D(\mathbf{M}_q)$ ), in this new case they are taken so as  $D(\mathbf{M}_p) \neq D(\mathbf{M}_q)$ . To illustrate this situation, the matrices  $\mathbf{M}_A$  and  $\mathbf{M}_D$  can be considered. They present the same IPP but they show different CP. In this example,  $\mathbf{M}_A$  has no dichroic elements while  $\mathbf{M}_D$  is constructed by using a horizontal polarizer as one of the components (Note that  $\mathbf{M}_A$  and  $\mathbf{M}_D$  represent very different systems). The same situation can be also reached with matrices  $\mathbf{M}_B$  and  $\mathbf{M}_C$ , to be compared with  $\mathbf{M}_E$  and  $\mathbf{M}_F$ , respectively (see Table 1). These examples correspond to the limiting case where one of the systems has no dichroic content, so they satisfy the condition  $D(\mathbf{M}_p) \neq D(\mathbf{M}_q)$ .

In the previous example, one of the systems in the couple did not have a dichroic component; however, the latter is not a mandatory condition since, as previously discussed, the same situation,

$(D(\mathbf{M}_p) \neq D(\mathbf{M}_q))$  can also be observed when considering two depolarizers with non-negligible but different dichroic content. These types of structures can be synthesized from Eq. (17) with  $\alpha_2 = \alpha_4 = 0$  by properly selecting the values of  $\alpha_1$  and  $\alpha_3$ . Note that after normalizing the sum of the  $\alpha_i$  weights to 1 ( $\sum \alpha_i = 1$ ),  $\alpha_3 = (1 - \alpha_1)$ . Therefore, by modifying the value of  $\alpha_1$  it is possible to build a collection of depolarizers with *a-priori* different  $P_{\Delta}$ , i.e. with different overall depolarizing power.

The values for  $P_{\Delta}$  (Fig. 4(a)), IPP (Fig. 4(a)), and CP (Fig. 4(b)) as respective functions of  $\alpha_1$  are graphically represented in Fig. 4. Figure 4(a) reveals that, by using this construction, there is an indeterminacy between two possible configurations with equal  $P_{\Delta}$  due to the presence of a minimum in the function (see the red horizontal line for the particular case  $P_{\Delta} = 0.64$ ). This ambiguity is also observed when using the IPP. In fact, the  $P_1$  function also presents a minimum, so that each possible  $P_1$  value is always associated with two different depolarizers (except for the minimum value); these two depolarizers being indistinguishable by means of  $P_1$  alone (see the orange curve in Fig. 4(a)). Therefore, the two parameters  $P_{\Delta}$  and  $P_1$ , do not provide discrimination for this set of depolarizers. In addition,  $P_2$  and  $P_3$  are always constant and equal to one.

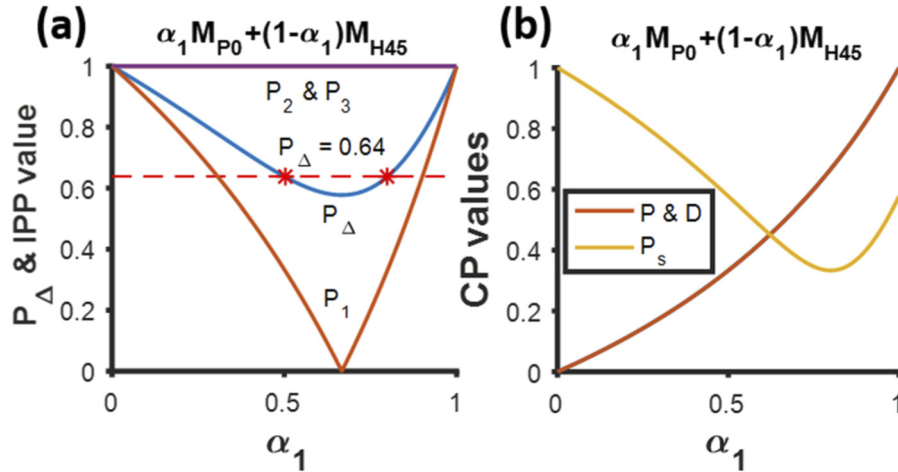


**Fig. 4.** Graphic representation of (a)  $P_{\Delta}$ , IPP and (b) CP as a function of  $\alpha_1$ . The matrices refer to Eq. (17) with  $\alpha_2 = \alpha_4 = 0$  and the red horizontal line represents the particular case  $P_{\Delta} = 0.64$ .

The above-mentioned ambiguity is lifted by using  $P$ - $D$ - $P_s$  space where  $P$  and  $D$  curves are not degenerate but are bijectively valued with respect to  $\alpha_1$ . Therefore, the  $P$ - $D$ - $P_s$  space allows deciding which element (dichroic or birefringent) is more significant in the weighted sum (see Fig. 4(b), since both  $P$  and  $D$  parameter functions do not present a minimum and so, there is no ambiguity between the elements of the depolarizer set).

From all possible depolarizers generated by Eq. (17) with  $\alpha_2 = \alpha_4 = 0$  we select two particular ones,  $\mathbf{M}_G$  ( $\alpha_1 = 0.5$ ) and  $\mathbf{M}_I$  ( $\alpha_1 = 0.8$ ), with identical  $P_{\Delta}$  value ( $P_{\Delta} = 0.64$ ) to be represented in the  $P$ - $D$ - $P_s$  space of Fig. 5. Their respective IPP, CP and  $P_{\Delta}$  values are presented in Table 1 and their  $\mathbf{M}$  are given in the Table S1 of the Supplement 1. Note that both depolarizers are represented by the same point in the IPP space ( $P_1 = 0.33$ ,  $P_2 = 1$  and  $P_3 = 1$ ) but lie at different points located on the surface  $P_{\Delta} = 0.64$  in the  $P$ - $D$ - $P_s$  space (red and pink points in the  $P = D$  plane).

Up to this point, we have discussed a group of depolarizing media satisfying  $D = P$ . In the following, we discuss depolarizing media satisfying  $D \neq P$ . In order to construct these types of depolarizers, at least two different dichroic elements are needed.  $\mathbf{M}_I$  is an example of a

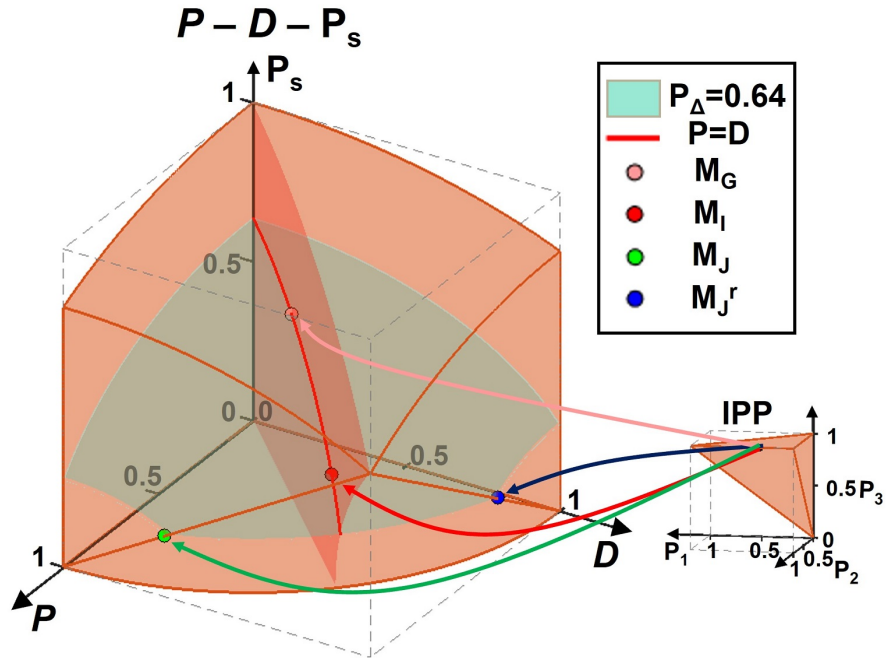


**Fig. 5.** Representation of the connection between the IPP space and the  $P$ - $D$ - $P_S$  space for the case of a group of depolarizers located in a single spot in the IPP space but distributed over a surface at the  $P$ - $D$ - $P_S$  space. The particular case of depolarizers having  $P_{\Delta}=0.64$  is presented as an illustrative example.

depolarizer with different  $D$  and  $P$  values (IPP, CP and  $P_{\Delta}$  values are shown in Table 1), built according to another generator given by Eq. (18). It is similar to the one in Eq. (17) but  $\mathbf{M}_{H0}$  is replaced by the non-depolarizing dichroic element  $\mathbf{M}_{P0} \cdot \mathbf{M}_{H45}$ :

$$\mathbf{M} = \alpha_1 \mathbf{M}_{P0} + \alpha_2 (\mathbf{M}_{P0} \cdot \mathbf{M}_{H45}) + \alpha_3 \mathbf{M}_{H45} + \alpha_4 (\mathbf{M}_{H45} \cdot \mathbf{M}_{H0}) \quad (18)$$

The construction of  $\mathbf{M}_J$  is summarized in Table 1 and its  $\mathbf{M}$  is provided in the Table S1 of the Supplement 1.

Given a Mueller matrix  $\mathbf{M}_J$ , the *reverse Mueller matrix*  $\mathbf{M}_J^r$  corresponds to the one obtained if the original incident and emerging polarizations are interchanged [26,35]. The construction of  $\mathbf{M}_J^r$ , together with the corresponding IPP, CP and  $P_{\Delta}$  values, are reported in Table 1. Note that  $\mathbf{M}_J$  and  $\mathbf{M}_J^r$  have identical  $P_{\Delta}$  and IPP, but different CP. These two systems are represented in the  $P$ - $D$ - $P_S$  space of Fig. 5 by blue and green dots, respectively. We observe that they lie over the same  $P_{\Delta}=0.64$  ellipsoid, and they are symmetrically located with respect to the  $D = P$  plane. In fact, the latter observation is not specific to the indicated example but it can be generalized to any pair of forward-reverse ( $\mathbf{M}$  and  $\mathbf{M}^r$ ) pairs of depolarizing systems. Therefore, the  $P$ - $D$ - $P_S$  space can be divided into two sub-spaces split by the  $D = P$  plane, each representing pairs of direct and reverse depolarizers. Such pairs of depolarizers share identical IPP but can be differentiated using the  $P$ - $D$ - $P_S$  space (Fig. 5). Conversely, IPP space has no potential to discriminate between forward and reverse systems, because their capabilities to depolarize (or polarize) an input beam are equivalent [36,37].

#### 4. Conclusions

In summary, in this work, we highlighted the usefulness and the physical significance of considering both the IPP and  $P$ - $D$ - $P_S$  spaces as complementary tools to completely describe the integral depolarization properties of material media, this approach providing global and fundamental information on depolarizers. On one hand, the IPP space provides information about the type of randomness induced by the sample. Importantly, unlike other depolarization bases, IPP are able to determine depolarization anisotropies induced by samples, i.e., if different input polarizations are differently depolarized. On the other hand, the  $P$ - $D$ - $P_S$  space, which is sensitive to the effects of dichroism and birefringence involved in the depolarizing process, brings information about the physical nature and other possible physical properties of the sample, related to  $P$ ,  $D$  and  $P_S$ .

As a general approach, when an unknown depolarizing medium must be characterized, the use of both IPP and  $P$ - $D$ - $P_S$  spaces together is recommended because, as discussed, they cover two different and complementary physical properties of depolarizers. Furthermore, the combined use of the IPP and  $P$ - $D$ - $P_S$  spaces constitutes a complete description of the depolarizing properties of the medium, and the use of no additional descriptor is required. Depending on the particular depolarizing medium under study, one of the two characteristic spaces may lead to better discrimination, as was shown through the study of a series of limiting cases where only one of the two spaces was able to discriminate between two differently constructed depolarizers. Moreover, in the general case where both spaces provide complementary information on depolarization properties, an observed tendency is that the IPP space provides better discrimination for depolarizers with values of  $P_A$  ranging between  $0.2 < P_A < 0.6$  whereas the  $P$ - $D$ - $P_S$  space performs better for depolarizing media with  $P_A > 0.6$ .

We believe that the methods described in this article constitute a significant step in the physical interpretation of the polarimetric response of depolarizing systems and provide analytical means to study depolarization processes. Given the great importance that depolarization measurements are taking in polarimetric imaging, this study is likewise relevant for the correct interpretation of the physical mechanisms causing depolarization in different kinds of samples.

**Funding.** Agència de Gestió d'Ajuts Universitaris i de Recerca (SGR 2017-00150); Ministerio de Economía y Competitividad (Fondos FEDER, RTI2018-097107-B-C31).

**Disclosures.** The authors declare no conflicts of interest related to this article.

**Data availability.** No data were generated or analyzed in the presented research.

**Supplemental document.**

**Supplemental document.** See [Supplement 1](#) for supporting content.

#### References

1. S. Cloude, *Polarisation: Applications in Remote Sensing* (Oxford Scholarship Online, 2010).
2. A. A. Kokhanovsky, *Light Scattering Reviews 10* (Springer Praxis Books, 2016).
3. J. Hough, "Polarimetry: a powerful diagnostic tool in astronomy," *Astron Geophys* **47**(3), 31–35 (2006).
4. B. Benneke, H. A. Knutson, J. Lothringer, I. J. M. Crossfield, J. I. Moses, C. Morley, L. Kreidberg, B. J. Fulton, D. Dragomir, A. W. Howard, I. Wong, J.-M. Désert, P. R. McCullough, E. M.-R. Kempton, J. Fortney, R. Gilliland, D. Deming, and J. Kammer, "A sub-neptune exoplanet with a low-metallicity methane-depleted atmosphere and mie-scattering clouds," *Nat Astron* **3**(9), 813–821 (2019).
5. V. V. Tuchin, *Tissue Optics: Light Scattering Methods and Instruments for Medical Diagnosis* (SPIE, 2007).
6. A. Van Eeckhout, A. Lizana, E. Garcia-Caurel, J. J. Gil, A. Sansa, C. Rodríguez, I. Estévez, E. González, J. C. Escalera, I. Moreno, and J. Campos, "Polarimetric imaging of biological tissues based on the indices of polarimetric purity," *J. Biophotonics* **11**(4), e201700189 (2018).
7. Y. Dong, H. He, W. Sheng, J. Wu, and H. Ma, "A quantitative and non-contact technique to characterise microstructural variations of skin tissues during photo-damaging process based on mueller matrix polarimetry," *Sci. Rep.* **7**(1), 14702 (2017).
8. M. Kupinski, M. Boffety, F. Goudail, R. Ossikovski, A. Pierangelo, J. Rehbinder, J. Vizet, and T. Novikova, "Polarimetric measurement utility for pre-cancer detection from uterine cervix specimens," *Bio. Opt. Exp.* **9**(11), 5691–5702 (2018).

9. B. Liu, Y. Yao, R. Liu, H. Ma, and L. Ma, "Mueller polarimetric imaging for characterizing the collagen microstructures of breast cancer tissues in different genotypes," *Opt. Commun.* **433**, 60–67 (2019).
10. F. Shen, M. Zhang, K. Guo, H. Zhou, Z. Peng, Y. Cui, F. Wang, J. Gao, and Z. Guo, "The depolarization performances of scattering systems based on the Indices of Polarimetric Purity (IPPs)," *Opt. Express* **27**(20), 28337–28349 (2019).
11. D. Li, K. Guo, Y. Sun, X. Bi, J. Gao, and Z. Guo, "Depolarization Characteristics of Different Reflective Interfaces Indicated by Indices of Polarimetric Purity (IPPs)," *Sensors* **21**(4), 1221 (2021).
12. D. Li, C. Xu, M. Zhang, X. Wang, K. Guo, Y. Sun, J. Gao, and Z. Guo, "Measuring glucose concentration in a solution based on the indices of polarimetric purity," *Biomed. Opt. Express* **12**(4), 2447–2459 (2021).
13. P. Wang, D. Li, X. Wang, K. Guo, Y. Sun, J. Gao, and Z. Guo, "Analyzing Polarization Transmission Characteristics in Foggy Environments Based on the Indices of Polarimetric Purity," *IEEE Access* **8**, 227703–227709 (2020).
14. J. J. Gil and E. Bernabeu, "Depolarization and polarization indices of an optical system," *Opt. Acta* **33**(2), 185–189 (1986).
15. S. R. Cloude, "Group theory and polarisation algebra," *Optik* **75**, 26–36 (1986).
16. R. A. Chipman, "Depolarization index and the average degree of polarization," *Appl. Opt.* **44**(13), 2490–2495 (2005).
17. R. Ossikovski, "Analysis of depolarizing mueller matrices through a symmetric decomposition," *J. Opt. Soc. Am. A* **26**(5), 1109–1118 (2009).
18. R. Ossikovski, "Alternative depolarization criteria for mueller matrices," *J. Opt. Soc. Am. A* **27**(4), 808–814 (2010).
19. R. Espinosa-Luna, E. Bernabeu, and G. Atondo-Rubio, "Q(m) and the depolarization index scalar metrics," *Appl. Opt.* **47**(10), 1575–1580 (2008).
20. I. S. José and J. J. Gil, "Invariant indices of polarimetric purity: Generalized indices of purity for nxn covariance matrices," *Opt. Commun.* **284**(1), 38–47 (2011).
21. J. J. Gil, "Components of purity of a mueller matrix," *J. Opt. Soc. Am. A* **28**(8), 1578–1585 (2011).
22. A. Tariq, P. Li, D. Chen, D. Lv, and H. Ma, "Physically realizable space for the purity-depolarization plane for polarized light scattering media," *Phys. Rev. Lett.* **119**(3), 033202 (2017).
23. A. Tariq, H. He, P. Li, and H. Ma, "Purity-depolarization relations and the components of purity of a Mueller matrix," *Opt. Express* **27**(16), 22645–22662 (2019).
24. R. Ossikovski and J. Vizet, "Eigenvalue-based depolarization metric spaces for mueller matrices," *J. Opt. Soc. Am. A* **36**(7), 1173–1186 (2019).
25. C. J. R. Sheppard, A. Bendandi, A. L. Gratiet, and A. Diaspro, "Eigenvectors of polarization coherency matrices," *J. Opt. Soc. Am. A* **37**(7), 1143–1154 (2020).
26. J. J. Gil and R. Ossikovski, *Polarized Light and the Mueller Matrix Approach* (CRC, 2016).
27. J. J. Gil, "Structure of polarimetric purity of a mueller matrix and sources of depolarization," *Opt. Commun.* **368**, 165–173 (2016).
28. J. J. Gil, "Transmittance constraints in serial decompositions of depolarizing Mueller matrices. The arrow form of a Mueller matrix," *J. Opt. Soc. Am. A* **30**(4), 701–707 (2013).
29. J. J. Gil, "Polarimetric characterization of light and media," *Eur. Phys. J. Appl. Phys.* **40**(1), 1–47 (2007).
30. J. J. Gil, "Characteristic properties of Mueller matrices," *Eur. Phys. J. Appl. Phys.* **17**(2), 328–334 (2000).
31. J. J. Gil, "On optimal filtering of measured Mueller matrices," *Appl. Opt.* **55**(20), 5449–5455 (2016).
32. A. Van Eeckhout, A. Lizana, E. Garcia-Caurel, J. J. Gil, R. Ossikovski, and J. Campos, "Synthesis and characterization of depolarizing samples based on the indices of polarimetric purity," *Opt. Lett.* **42**(20), 4155–4158 (2017).
33. G. Soriano, M. Zerrad, and C. Amra, "Enpolarization and depolarization of light scattered from chromatic complex media," *Opt. Express* **22**(10), 12603–12613 (2014).
34. Y. Xu, Z. Wang, and W. Zhang, "Depolarization effect in light scattering of a single gold nanosphere," *Opt. Express* **28**(16), 24275–24284 (2020).
35. Z. Sekera, "Scattering Matrices and Reciprocity Relationships for Various Representations of the State of Polarization," *J. Opt. Soc. Am. A* **56**(12), 1732–1740 (1966).
36. A. Schönhofer and H. G. Kuball, "Symmetry properties of the mueller matrix," *Chem. Phys.* **115**(2), 159–167 (1987).
37. J. J. Gil, "Invariant quantities of a mueller matrix under rotation and retarder transformations," *J. Opt. Soc. Am. A* **33**(1), 52–58 (2016).